Three-Dimensional Dual-Band Dielectric Resonator Antenna for Wireless Communication

SHAILESH MISHRA [1], (Member, IEEE), SUSHRUT DAS[1], (Senior Member, IEEE), SHYAM SUNDAR PATTNAIK[2], (Senior Member, IEEE), SACHIN KUMAR [3], AND BINOD KUMAR KANAUJIA [4], (Senior Member, IEEE)

[1]Department of Electronics Engineering, Indian Institute of Technology (Indian School of Mines), Dhanbad 826004, India
[2]Department of ETV, National Institute of Technical Teachers Training and Research, Chandigarh 160019, India
[3]School of Electronics Engineering, Kyungpook National University, Daegu 41566, South Korea
[4]School of Computational and Integrative Sciences, Jawaharlal Nehru University, New Delhi 110067, India

Corresponding author: Shailesh Mishra (mishrashail1@gmail.com)

ABSTRACT A three-dimensional dual-band dielectric resonator antenna, comprised of five rectangular dielectric resonator (RDR) radiating elements, is proposed for wireless communication applications. The presented multiple-input-multiple-output (MIMO)/diversity antenna system use $TE_{1\delta1}^{Y}$ and $HEM_{2\delta1}$ modes of the RDR antenna for the transmission/reception of data. The $TE_{1\delta1}^{Y}$ mode covers the frequency range from 3.3 to 3.8 GHz, covering Wi-MAX, sub-6 GHz, and LTE (3.41-3.5 GHz uplink/3.51-3.6 GHz downlink) 5G application bands. The $HEM_{2\delta1}$ mode covers Wi-Fi (5.725-5.875 GHz) and ITS 5.9 GHz (5.875-5.925 GHz) bands. The five RDR antenna elements are excited through coaxial feeds and are arranged in a cubical fashion to cover all directions, except −Z direction. The RDR elements are oriented and positioned to achieve a minimum correlation between the radiating elements. The proposed antenna exhibits a gain of 7 dB in the lower band while 7.2 dB gain is obtained in the upper band.

INDEX TERMS DRA, isolation, MIMO, pattern diversity.

I. INTRODUCTION

Microstrip antennas have low radiation efficiency, high conductive loss, and requirement of complicated excitation techniques. Therefore, dielectric resonator antennas (DRAs) are often used as a substitute for microstrip antennas [1]. High gain and wide / multiple bandwidth can be achieved using DRAs by changing the dimensions, permittivity, and feeding of the dielectric material. In [2], dual-band and triple-band characteristics were achieved using the T-matched dipole/loop excitation and characteristic mode analysis. In addition to it several other feeding techniques like strip [3], aperture coupled [4], differential microstrip [5], coplanar waveguide [6], and probe [7] feeds have been reported for the DRA. Also, different DRA shapes, such as hemispherical [7], rectangular [8], cylindrical [9], hexagonal [10], and ring rod [11] have been investigated. Among them the rectangular DRA (RDRA) offers one extra degree of freedom and it also shows minimum cross-polarization in contrast to the cylindrical shape of the dielectric resonator [12]–[14].

The associate editor coordinating the review of this manuscript and approving it for publication was Pietro Savazzi.

TABLE 1. Design parameters of the cubical multi-antenna system.

Parameter	Value in mm	Parameter	Value in mm
h	1.57	DR_X	17.38
H_F	5.4	DR_Y	14.12
L_{SUB}	60	DR_Z	9.61
W_{SUB}	60	a	62

A high permittivity dielectric material can be used to reduce the size of DRA, but it deteriorates the impedance bandwidth and radiation efficiency of the antenna. The introduction of symmetrical perfect electric conductor (PEC) plane also offers size reduction, where electric flux lies perpendicular to the PEC plane [15]. The coaxial probe works as a vertical current source and positioned for the maximum electric field to excite modes in the RDRA. The excited modes can be changed by varying the coordinate of the coaxial feed. The desired resonance frequency can be adjusted by optimizing the length and position of the feeding probe [13].

In MIMO systems the channel capacity can be increased by increasing the number of radiating elements. However, it will
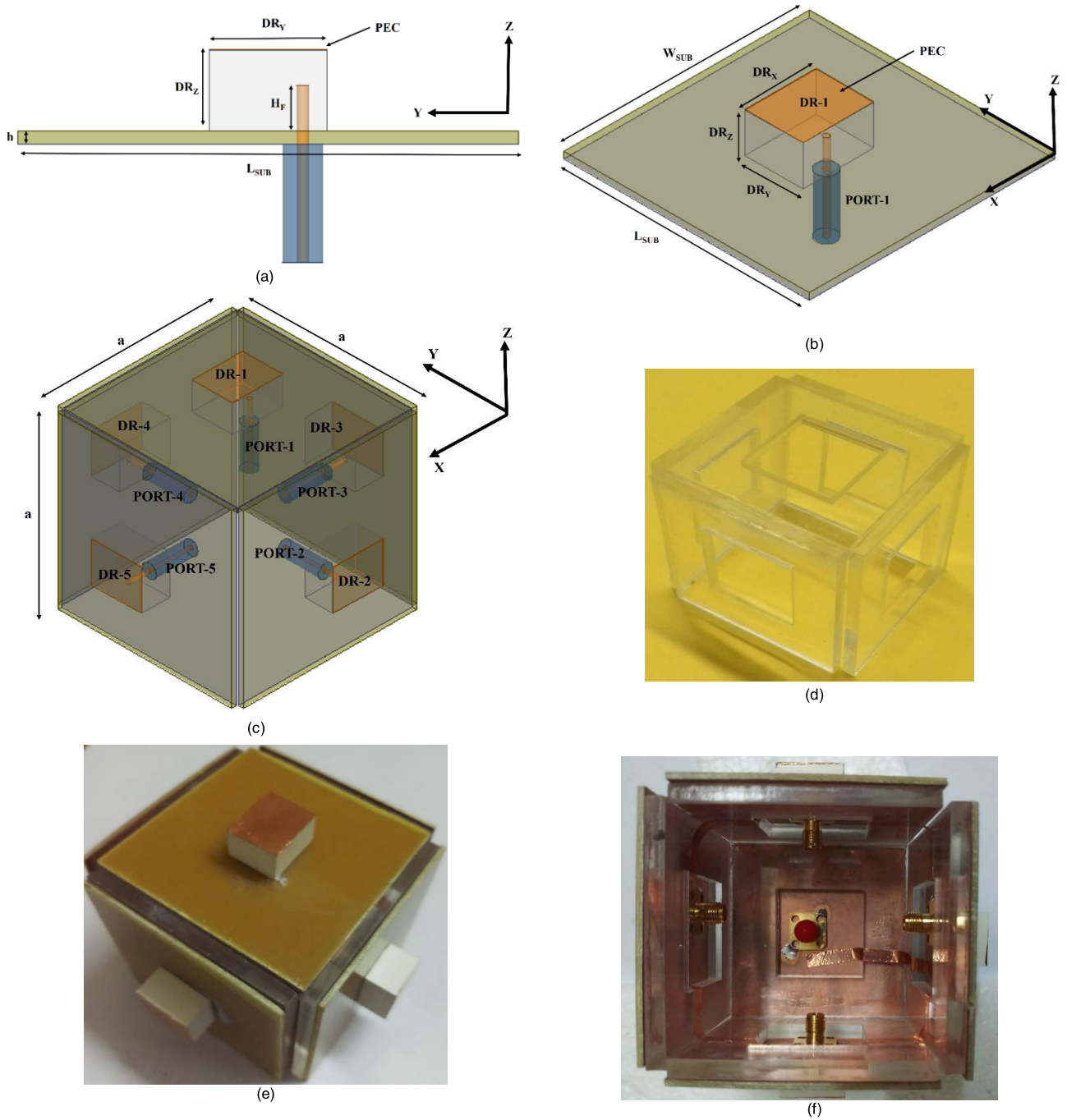
FIGURE 1. Antenna configuration (a) side view of the RDRA element, (b) top view of the RDRA element, (c) isometric view of the MIMO, (d) acrylic box, (e) MIMO antenna prototype, and (f) inner view of the MIMO antenna with connected ground planes.

also increase the antenna footprint. Therefore, in order to limit the antenna footprint, a 3D geometry may be exploited. In [16], a 3D single-band diversity antenna was proposed for 1.45 GHz applications. The antenna is composed of three monopoles, a defected ground structure, and a complex decoupling structure. The monopoles were arranged on a circular ground plane at a mutual angle of 120° and the complex decoupling structure was placed symmetrically in between them. The complex decoupling structure restricted the space wave whereas the DGS restricted the surface wave to obtain high isolation.

Recently multiple-input-multiple-output (MIMO)/diversity technology is used by different wireless communication systems for increasing data rate and throughput. The diversity techniques are used to mitigate multipath fading and improve the quality and reliability of a high-speed wireless
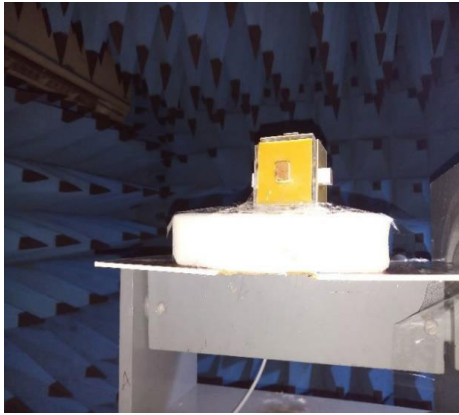
FIGURE 2. Measurement setup.

channel. MIMO systems are widely used for IEEE802.11n (WLAN) and IEEE 802.16 (Wi-MAX) standards to obtain better signal quality and high data transmission rate. Recently, various dual-band MIMO DRAs have been proposed to cover different wireless communication bands or standards. However, isolation improvement between the radiators is still a challenge [14].

In this article, a five-port RDRA MIMO configuration is presented for Wi-MAX, sub-6 GHz, 5G LTE (3.41-3.5 GHz uplink/3.51-3.6 GHz downlink), Wi-Fi (5.725-5.875 GHz) and ITS (5.875-5.925 GHz) application bands. The five RDRA elements are placed orthogonally (in XY-, YZ- and XZ-planes) and excited using coaxial feeds. This kind of arrangement, due to the multi-directional pattern, reduces mutual coupling between the RDRA ports. A PEC layer is deposited on the top of each RDRA element which reduces the size of the MIMO system by exciting suitable modes. The ground planes of the five RDRA elements are connected through a copper tape that offers a common reference voltage level to all the radiating elements. To examine the diversity performance of RDR based cubical antenna, the channel correlation is checked by envelope correlation coefficient (ECC) and gain performance for the different wireless environments is evaluated by the mean effective gain (MEG). Besides this, other parameters such as channel capacity loss (CCL), total active reflection coefficient (TARC), and diversity gain (DG) are also presented. A stable gain, directive radiation patterns, and low ECC are obtained for the proposed RDR-based 3D MIMO antenna system. Modelling and analysis of the diversity sub-system are presented in section-II while the analysis of results is presented in section-III. MIMO/diversity performance is analyzed in section-IV and the conclusion is presented in section-V.

II. CUBICAL ANTENNA MODELLING

The side view of the RDRA element is delineated in Fig. 1(a) and its isometric view in Fig. 1(b). An offset hole is introduced in the DRA element (in Y direction) to excite it by coaxial feed. The RDRA (ε_r =12) with a probe feed
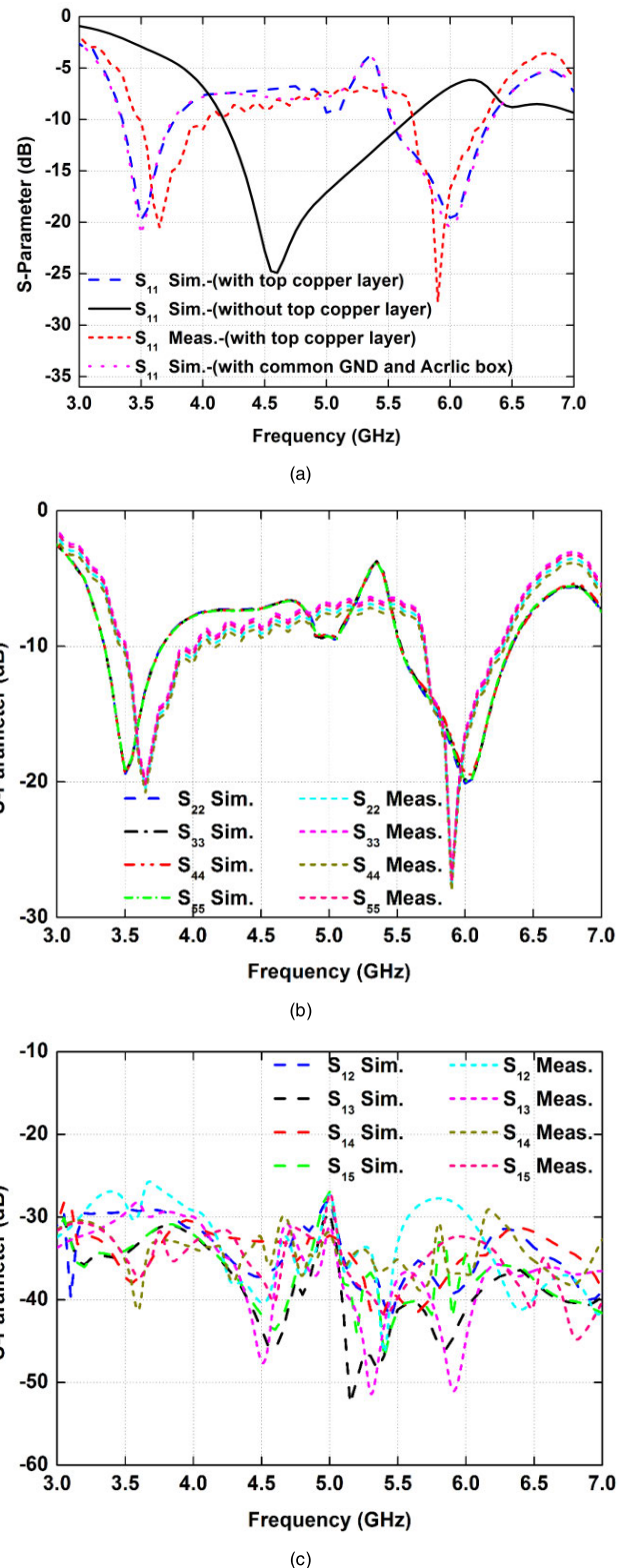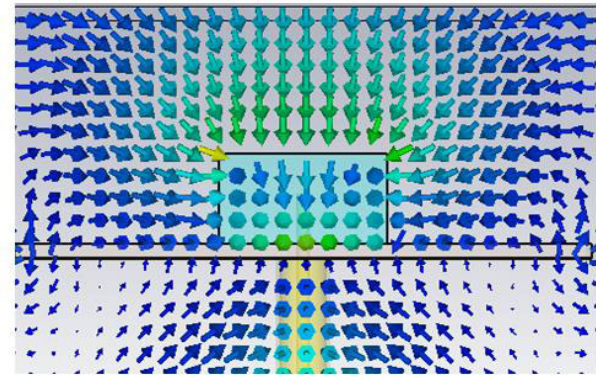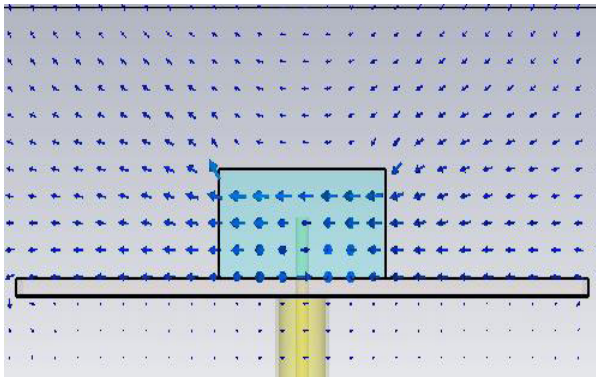

(a)

(b)

(c)

FIGURE 3. Scattering parameters (a) reflection coefficients at port-1 (b) reflection coefficients at ports 2-5 (c) transmission coefficients between different ports.
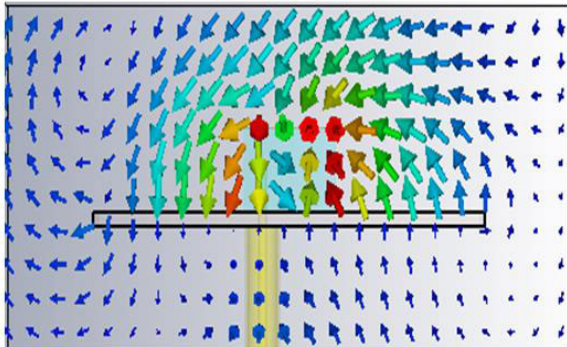
arrangement is placed on the FR-4 substrate ($\varepsilon_r^{SUB} = 4.4$) of thickness 1.57 mm. A copper layer is deposited on the top of the RDRA to excite suitable modes for dual-band resonance.

(a) XZ-plane (E-field)

(b) XZ-plane (H-field)

(c) YZ-plane (E-field)

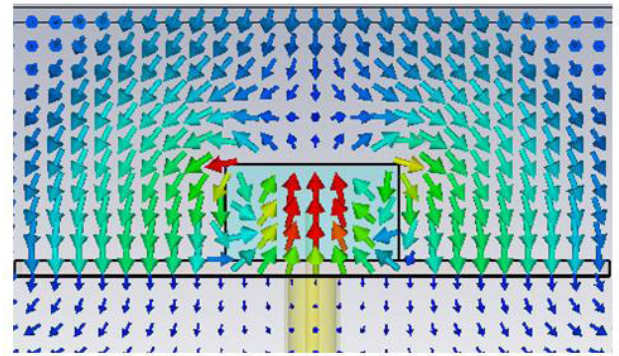**FIGURE 4.** Electric and magnetic field distributions within RDRA at 3.5 GHz.

(a) XZ-plane (E-field)

(b) XZ-plane (H-field)

(c) YZ-plane (E-field)

FIGURE 5. Electric and magnetic field distributions within RDRA at 5.9 GHz.

The resonant frequency of the RDR radiator is calculated using [17]

$$f_o = \frac{c}{2\pi \sqrt{\mu_r \varepsilon_r}} \sqrt{k_x^2 + k_y^2 + k_z^2} \tag{1}$$
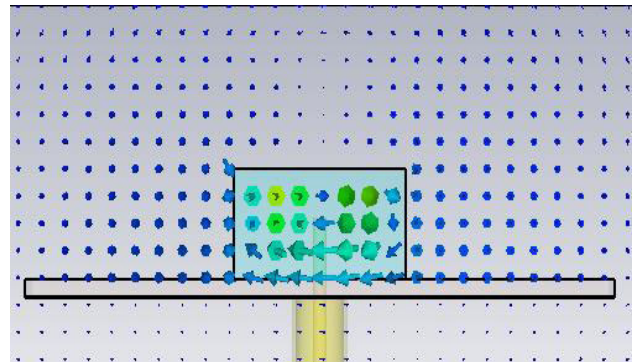
which is found by solving transcendental equations for TE^x and TE^y modes.

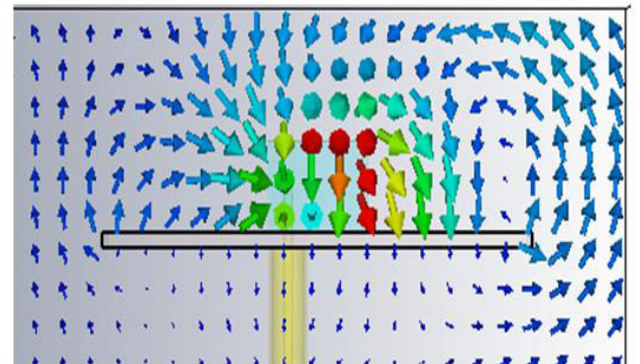$$k_x * \tan\left(\frac{k_x * D_{Yeff}}{2}\right) = \sqrt{(\varepsilon_r - 1) * k_0^2 - k_x^2} \tag{2}$$

$$k_y * \tan\left(\frac{k_y * D_{Xeff}}{2}\right) = \sqrt{(\varepsilon_r - 1) * k_0^2 - k_y^2} \tag{3}$$

where $k_x = \frac{m\pi}{DR_X}$, $k_y = \frac{n\pi}{DR_Y}$, $k_z = \frac{p\pi}{2*DR_Z}$, $k_0 = \frac{\omega_0}{v} = \frac{2\pi f_o \sqrt{\mu_r \varepsilon_r}}{c}$ and $k_x^2 + +k_y^2 + k_z^2 = k_0^2$

The effective dimensions of the DRA are given by following relations [14]

$$D_{Xeff} = DR_X \left(1 - \frac{1}{\varepsilon_{eff}}\right) \tag{4}$$

$$D_{Yeff} = DR_Y \left(1 - \frac{1}{\varepsilon_{eff}}\right) \tag{5}$$

$$\varepsilon_{eff} = \frac{\varepsilon_r^{SUB} * h + \varepsilon_r * DR_Z}{h + DR_Z} \tag{6}$$
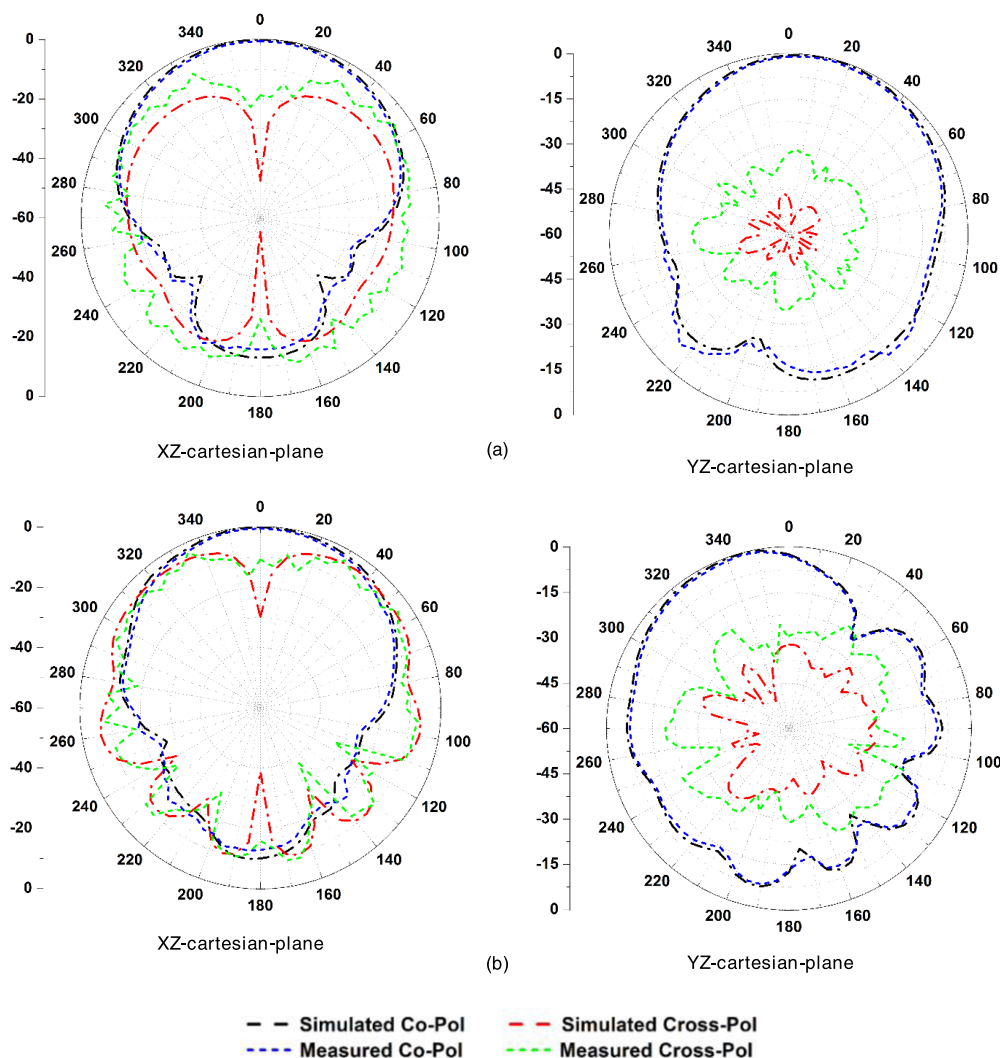
FIGURE 6. Normalized Co- and cross-pol radiation patterns of the RDR-1 antenna at (a) 3.5 GHz, (b) 5.9 GHz.

Five RDRA elements with dimensions 60 mm × 60 mm, are arranged in a cubical fashion to establish a multi-directional pattern, as shown in Fig. 1(c). An acrylic cubical box, shown in Fig. 1(d), was used to place the RDRA elements. The outer view of the fabricated five-port multi-antenna system is presented in Fig. 1(e). As shown in Fig. 1(f), the ground surfaces of all the RDRA elements are connected using conductive copper tape to implement a common ground. ANSYS HFSS and CST Microwave Studio simulators were used to design and analyze the dual-band MIMO antenna. The RDRA dimensions were optimized using the formulas in [14], [17]–[20] and are presented in Table 1.

III. RESULTS AND DISCUSSION
The radiation characteristics of the prototype MIMO sub-system were measured (Fig. 2) in anechoic-chamber. The antenna performance parameters were measured using Keysight N5221A PNA.

The transmission and reflection coefficient parameters of the RDRA are depicted in Fig. 3. Slight variations in measured and simulated results are due to the following factors: (i) fabrication tolerance of DRA structure and feed network, (ii) DRA cutting and mounting, (iii) variation in permittivity values due to FR-4 and DRA combination, (iv) adhesive material used to fix DRA to the ground plane, and (v) unwanted air gaps.

Comparison of the reflection coefficient responses of the RDRA, with and without the PEC layer, are provided in Fig. 3 (a). The figure reveals that the RDRA without PEC layer has single operating band at 4.6 GHz whereas the RDRA with PEC layer has two operating bands at 3.5 GHz and 5.9 GHz. Therefore the RDRA with the PEC layer has the lowest operating band at 3.5 GHz, compared to 4.6 GHz for an RDRA without the PEC layer. This corresponds to a 31.43% reduction in the size of the RDRA element. The size reduction can be explained with the excitation of suitable modes inside the RDR. If the RDR is mounted on a ground surface without
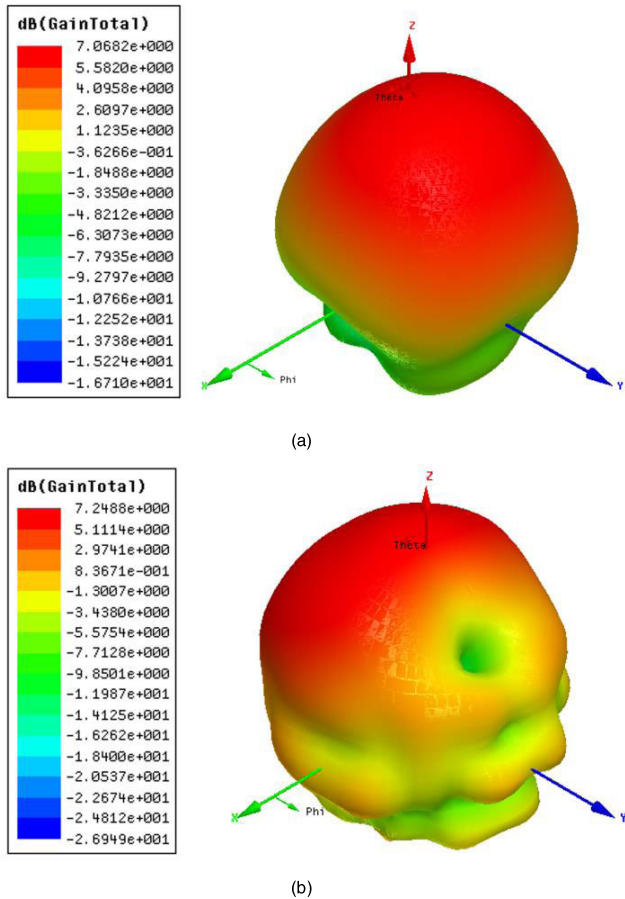
FIGURE 7. 3D radiation patterns of the RDR-1 antenna at (a) 3.5 GHz, (b) 5.9 GHz.

the PEC layer at the top, the *TE* modes are usually excited. But in the proposed design, the RDRA has two PEC boundaries (top and bottom) which makes the tangential electric flux zero at $Z = 0$ and $Z = DR_Z$, thereby exciting quasi-TE and hybrid HEM mode along with pure TE modes.

It may be noted that the proposed 3-D MIMO antenna is composed of five RDRA elements arranged in cubical fashion on an acrylic box, as shown in Fig. 1(d). The copper tape is used to connect the ground planes of the RDRA elements, as illustrated in Fig. 1(f). The effect of the acrylic box and the common ground plane on the proposed antenna is also shown in Fig. 3(a), where a small variation in the resonance frequency is noticed. The reflection coefficient curves for the RDR-2 to RDR-5 antennas are depicted in Fig. 3(b).

Fig. 3(c) depicts the simulated and measured transmission coefficients at ports-2 to −5 with respect to port-1 of the cubical multi-antenna system. The measured transmission coefficients between port-1 and other ports are below −25 dB for both the operating bands. The lower coupling can be explained as a result of the orthogonal placement of the RDRA elements.

To find out excited modes in the RDRA, the electric field distributions within it are shown in Fig. 4 and Fig. 5. The figures reveal that at 3.5 GHz, only X-component of the

magnetic field exists (Fig. 4(b)), which implies the existence of TE mode in the RDRA. From Figs. 5(a), (b) and (c), it is clear that all the electric and magnetic components (X, Y, and Z) are non-zero, which implies the existence of HEM mode at 5.9 GHz. Figs. 4(a), (b) and (c) shows $TE_{1\delta1}^{Y}$ mode field distributions at 3.5 GHz, whereas Figs. 5(a), (b) and (c) shows $HEM_{2\delta1}$ mode field distributions at 5.9 GHz. The theoretical resonance frequencies for these modes, as calculated from equations (1)-(6), are 3.54 GHz ($TE_{1\delta1}^{Y}$) and 5.92 GHz ($TE_{2\delta1}^{Y}$), respectively, which are very close to the simulated values.

Figs. 6(a) and (b) presents the simulated and measured radiation patterns of the DR-1 (positioned on XY-plane), on both orthogonal (X = 0 and Y = 0) planes at 3.5 GHz and 5.9 GHz, respectively. The figures depict that DR-1 radiates in the +Z direction at both the bands. The figures also reveal that the back lobe is more than 20 dB down on xz-plane and more than 15-dB down on the yz-plane at both frequencies, which signifies negligible radiation in the −Z direction. To confirm this the 3D radiation patterns of the antenna at both resonating frequencies are presented in Figs. 7(a) and (b) that depicts DR-1 radiates in the +Z direction and there is no radiation in the −Z direction.

The simulated and measured co-polarization and cross-polarization radiation patterns of RDR-2 and RDR-4 (positioned on XZ-plane) at 3.5 GHz and 5.9 GHz are shown in Figs. 8(a) and (b), respectively. For RDR-3 and RDR-5 (positioned at X = 0 plane), the radiation patterns at 3.5 GHz and 5.9 GHz are presented in Figs. 8(c) and (d), respectively. Fig. 8(a) depicts that RDR-2 is radiating in −Y direction, whereas Fig. 8(b) depicts that RDR-4 is radiating in +Y direction. Similarly, Figs. 8(c) and (d) depict −X and +X direction radiations from RDR-3 and RDR-5, respectively. Hence, the proposed MIMO antenna is capable to radiate in all directions except −Z direction.

Fig. 6 and Fig. 8 reveals a relatively high cross-pol, except at the direction of maximum radiation. This may be explained due to complex field distribution at higher modes. The cross-polarization can be improved by employing different techniques, such as, metal strip wrapping on rectangular DRA [21], perturbation using metallic post [22], [23], dielectric perturbation [24] etc.

The simulated and measured gain curves are compared in Fig. 9. The figure reveals that maximum measured gain of 7 dB is realized at 3.5 GHz and 7.2 dB gain is achieved at 5.9 GHz.

IV. MIMO CHARACTERISTICS

To evaluate the correlation effect of multi-antenna elements, the ECC is evaluated using the following relation [25]

$$\rho_{e_{ij}} = \frac{\left| \iint\limits_{4\pi} \left[\overrightarrow{F}_i (\theta, \varphi) * \overrightarrow{F}_j (\theta, \varphi) \right] d\Omega \right|^2}{\iint\limits_{4\pi} \left| \overrightarrow{F}_i (\theta, \varphi) \right|^2 d\Omega \iint\limits_{4\pi} \left| \overrightarrow{F}_j (\theta, \varphi) \right|^2 d\Omega} \quad (7)$$

XY-cartesian-plane at 3.5 GHz

XY-cartesian-plane at 3.5 GHz

YZ-cartesian-plane at 3.5 GHz

YZ-cartesian-plane at 3.5 GHz

XY-cartesian-plane at 5.9 GHz

XY-cartesian-plane at 5.9 GHz

YZ-cartesian-plane at 5.9 GHz

YZ-cartesian-plane at 5.9 GHz

(a) Port 2

(b) Port 4

FIGURE 8. Co- and Cross-polarization patterns of the RDRA elements (a) DR-2 in Z = 0 and X = 0 planes, (b) DR-4 in Z = 0 and X = 0 planes, (c) DR-3 in Z = 0 and Y = 0 planes, (d) DR-5 in Z = 0 and Y = 0 planes.

XY-cartesian-plane at 3.5 GHz

YZ-cartesian-plane at 3.5 GHz

XY-cartesian-plane at 5.9 GHz

YZ-cartesian-plane at 5.9 GHz

(c) Port 3

XY-cartesian-plane at 3.5 GHz

YZ-cartesian-plane at 3.5 GHz

XY-cartesian-plane at 5.9 GHz

YZ-cartesian-plane at 5.9 GHz
(d) Port 5

— — Simulated Co-Pol   — — Simulated Cross-Pol
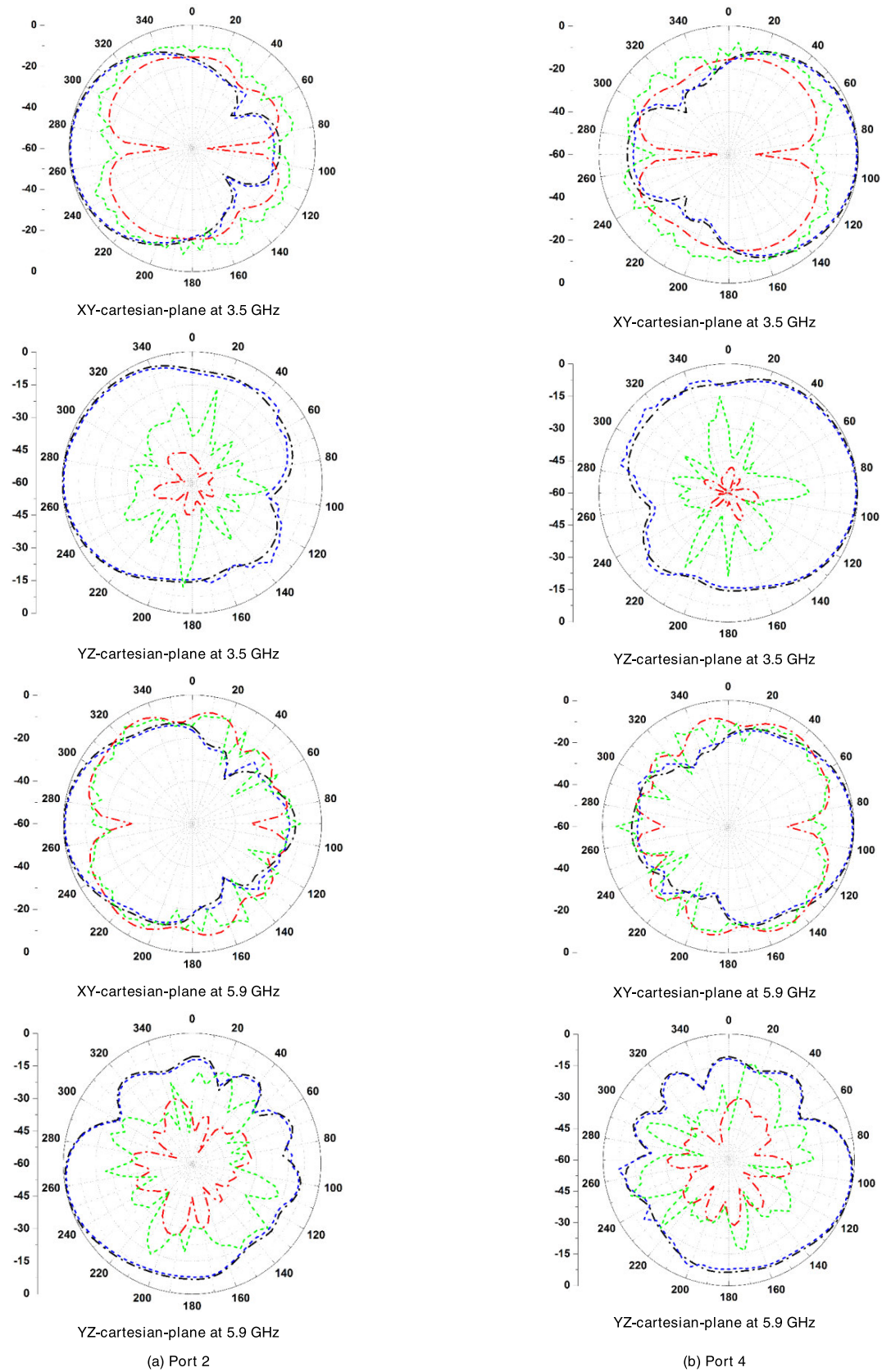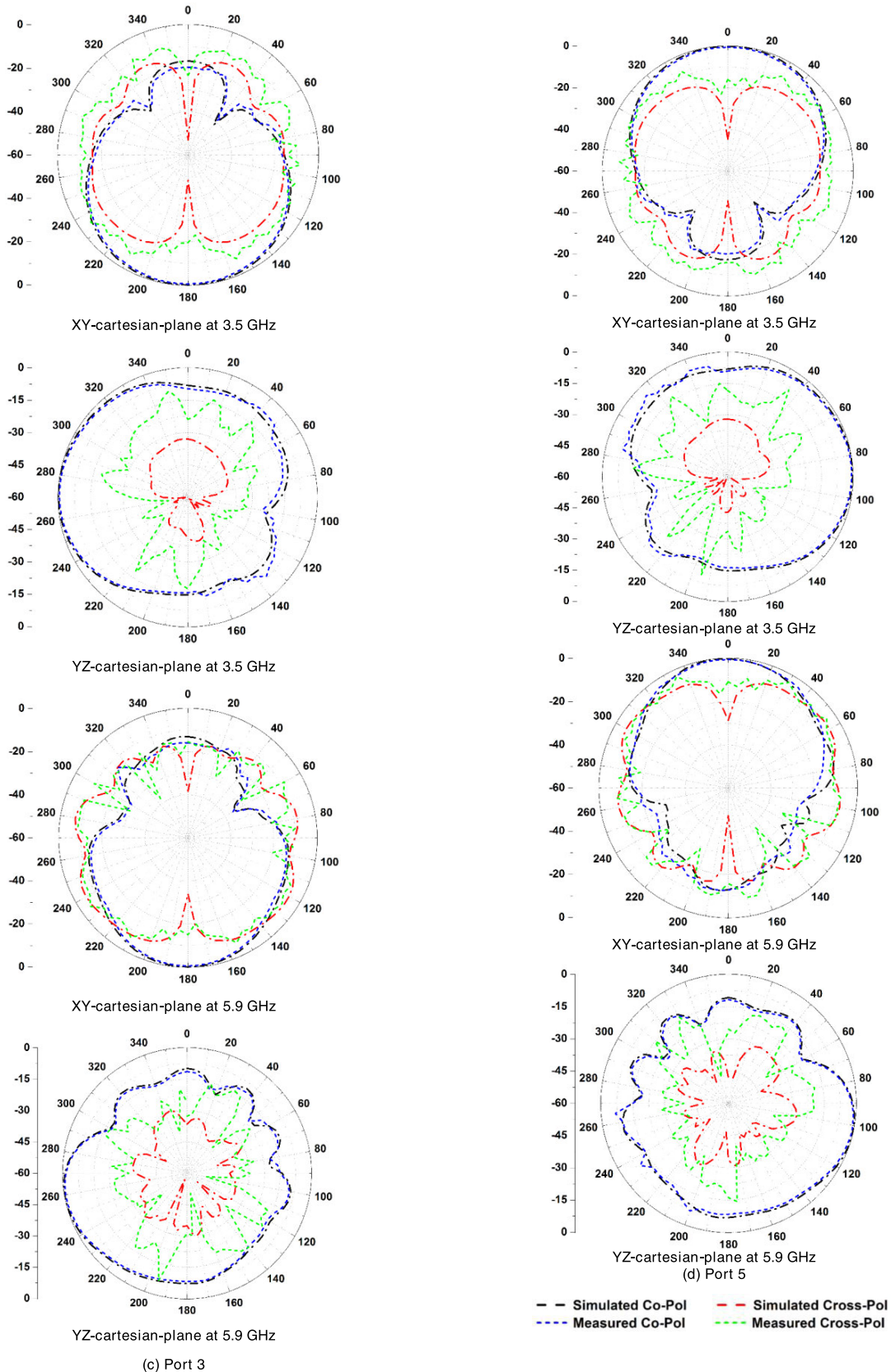— — Measured Co-Pol   — — Measured Cross-Pol

FIGURE 8. *(Continued.)* Co- and Cross-polarization patterns of the RDRA elements (a) DR-2 in Z = 0 and X = 0 planes, (b) DR-4 in Z = 0 and X = 0 planes, (c) DR-3 in Z = 0 and Y = 0 planes, (d) DR-5 in Z = 0 and Y = 0 planes.

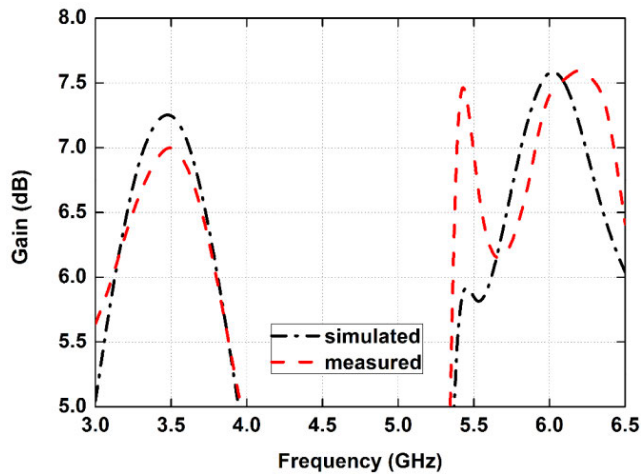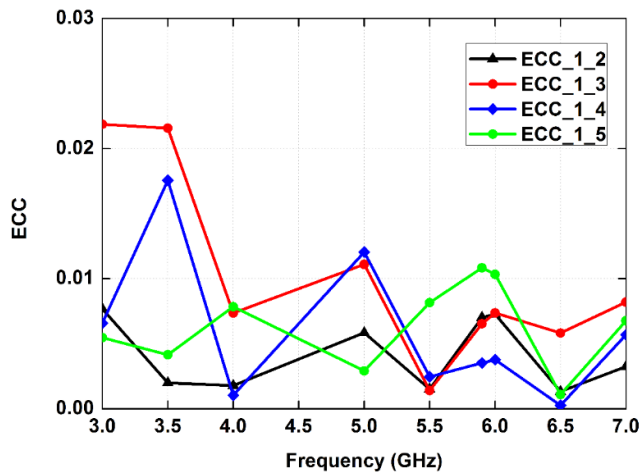**FIGURE 9.** Simulated and measured gain of the MIMO structure.

FIGURE 10. ECC curves of the cubical diversity antenna.

FIGURE 11. DG curves of the cubical MIMO antenna.
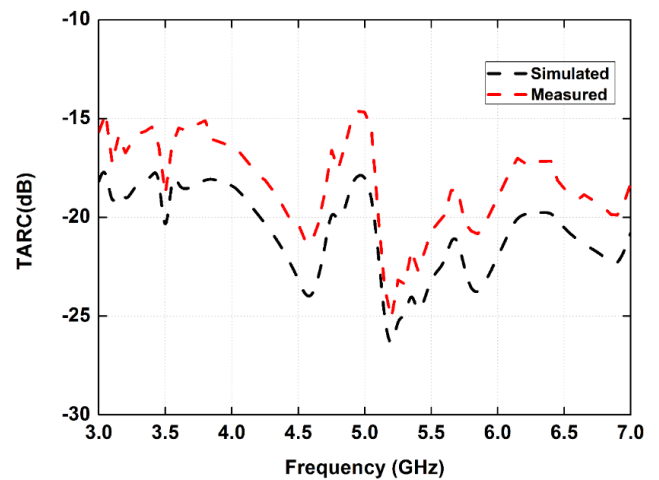
FIGURE 12. Simulated and measured TARC response.
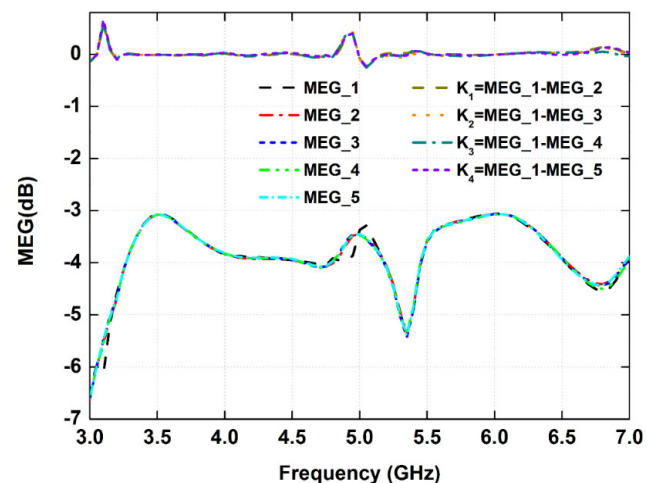
FIGURE 13. Power ratio (k) and MEG response.

where, $\overrightarrow{F_i}(\theta, \phi)$ is the radiated field of ith antenna element and $\overrightarrow{F_j}(\theta, \phi)$ is the radiated field of jth antenna element. Using this relation, the ECC of the cubical antenna is found and presented in Fig. 10. It confirms that ECC is less than 0.5 in the resonating band. The DG [26] of the suggested cubical antenna is determined by using the equation (8) and plotted in Fig. 11.

$$DG = 10\sqrt{1 - (ECC)^2} \qquad (8)$$

The parameter TARC [16] of the multi-port antenna system can be calculated using

$$TARC = \sqrt{\sum_{i=1}^{N} |b_i|^2} / \sqrt{\sum_{i=1}^{N} |a_i|^2} \qquad (9)$$

where, a_i and b_i represents the sending and receiving waves of the ith port, respectively. For the N-port system, all $N \times N$ scattering parameters are interrelated according to the relation

$$[b]_{N \times 1} = [S]_{N \times N} [a]_{N \times 1} \qquad (10)$$

The response due to highly isolated radiating elements is presented by the TARC curves in Fig. 12.
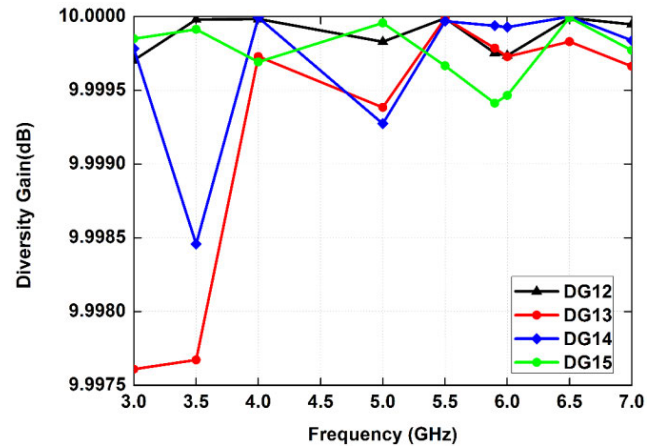
In a fading environment, the ratio of the power received by the diversity antenna and the isotropic radiator is known as

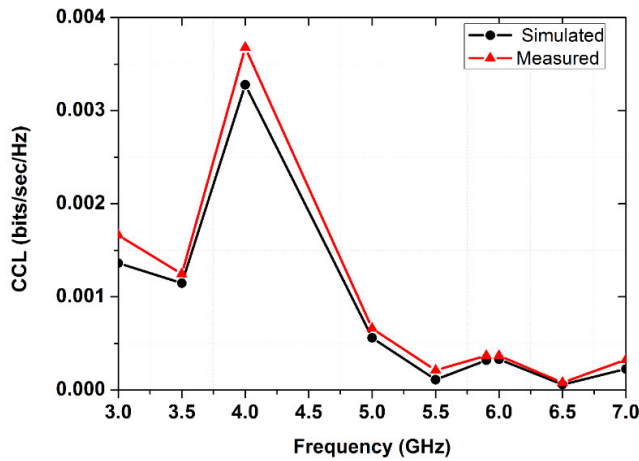**FIGURE 14.** Simulated and measured CCL curves.

TABLE 2. Proposed antenna Comparison with reported MIMO antenna structures.

Ref.	No. of Ports	Isolation (dB)	Bandwidth (GHz)	ECC	Volume ($\lambda_0 \times \lambda_0 \times \lambda_0$)
[1]	8	20	5.6-5.9	<0.25	0.84×0.52×0.84
[29]	18	20	2.4-2.8	---	0.76×0.76×0.76
[30]	6	25	3.12-5.88, 7.2-8.41	5×10^{-4}	1.27×1.27×0.62
[31]	8	12.5	2.55-2.65	<0.16	1.17×0.59×0.052
[32]	4	30	1.73-2.57	<0.012	0.81×0.81×1.14
This work	5	25	3.3-3.8, 5.5-6.3	<0.025	0.71×0.71×0.82

MEG [27]. For the ith antenna element, it can be evaluated by

$$\text{MEG}_i = 0.5 \left[1 - \sum_{j=1}^{N} |S_{ij}|^2 \right] \quad (11)$$

where $N = 1, 2, 3, 4, 5$. The difference between the MEG magnitudes (in dB) is known as the power ratio (k). Equation (12) represents that for good diversity performance the power ratio should be less than 3 dB.

$$k = |\text{MEG}_1 - \text{MEG}_2| < 3\text{dB} \quad (12)$$

Fig. 13 depicts the MEG of RDRA-based 3D MIMO antenna and power ratios with respect to the RDR-1 antenna element, which satisfies the required criteria of 1 [17]. Fig. 13 shows that MEG values are almost the same at operating bands (nearly equal to −3 dB).

CCL shows the peak transmission rate at which information signal can propagate uninterruptedly with minimum loss. The CCL can be computed as [28]

$$C = -\log_2 \det \left(\psi^R \right) \quad (13)$$

where ψ^R is the correlation matrix defined as

$$\psi^R = \begin{bmatrix} \rho_{11} & \rho_{12} & \rho_{13} & \rho_{14} & \rho_{15} \\ \rho_{21} & \rho_{22} & \rho_{23} & \rho_{24} & \rho_{25} \\ \rho_{31} & \rho_{32} & \rho_{33} & \rho_{34} & \rho_{35} \\ \rho_{41} & \rho_{42} & \rho_{43} & \rho_{44} & \rho_{45} \\ \rho_{51} & \rho_{52} & \rho_{53} & \rho_{54} & \rho_{55} \end{bmatrix} \quad (14)$$

For the cubical diversity antenna, CCL for the desired bands (shown in Fig. 14) is within the limit of 0.4 bits per second per hertz.

Table 2 presents a comparison of the proposed cubical MIMO antenna with some reported non-planar MIMO antennas based on bandwidth, number of ports, isolation level, correlation, and size of the antenna. The table reveals that the proposed cubical MIMO antenna exhibit dual-band characteristics with the smallest volume.

V. CONCLUSION

A cubical-shaped five-element MIMO antenna for LTE (3.41-3.5 GHz uplink/3.51-3.6 GHz downlink), WiMAX-(3.3 to 3.8 GHz), Wi-Fi (5.725-5.875GHz) and ITS 5.9 GHz (5.875-5.925 GHz) applications is presented in this paper. A PEC layer is deposited on the top of the RDRA elements and an offset coaxial probe feed excitation is used to obtain dual-band resonance with directional radiation characteristics. The MIMO RDRA ports have more than 25 dB isolation in both the operating bands due to the orthogonal placement of the radiating elements. The diversity performance parameters such as ECC, TARC, CCL, MEG, and DG are within the required limits, hence making the proposed diversity/MIMO antenna fit for wireless communication applications.

To the best of author's knowledge, the cubical-shaped DRA with PEC layer at the top and covering all directions except −Z direction is reported for the first time. It also shows that the use of the PEC layer at the top of the RDRA element shifts the operating band of the DRA towards the lower frequency, thus effectively reducing the size of the antenna.

It may be noted that the proposed antenna radiates in almost all directions (except the negative z-direction) with high isolation at the cost of space. However, the 3D MIMO antenna also has several advantages such as simplicity, increased channel capacity, high isolation, low antenna footprint etc. So the proposed 3D antenna has an inherent advantages for those applications where we require high channel capacity and isolation with limited antenna footprint, but the antenna volume is not of much concern (such as indoor communication, base station, and vehicular communication).

REFERENCES

[1] G. Das, N. K. Sahu, A. Sharma, R. K. Gangwar, and M. S. Sharawi, "Dielectric resonator-based four-element eight-port MIMO antenna with multi-directional pattern diversity," *IET Microw., Antennas Propag.*, vol. 13, no. 1, pp. 16–22, Jan. 2019.

[2] Q. Wu, "Characteristic mode assisted design of dielectric resonator antennas with feedings," *IEEE Trans. Antennas Propag.*, vol. 67, no. 8, pp. 5294–5304, Aug. 2019.

[3] B. Li and K. W. Leung, "Strip-fed rectangular dielectric resonator antennas with/without a parasitic patch," *IEEE Trans. Antennas Propag.*, vol. 53, no. 7, pp. 2200–2207, Jul. 2005.

[4] A. S. Al-Zoubi, A. A. Kishk, and A. W. Glisson, "Aperture coupled rectangular dielectric resonator antenna array fed by dielectric image guide," *IEEE Trans. Antennas Propag.*, vol. 57, no. 8, pp. 2252–2259, Aug. 2009.

[5] S.-J. Guo, L.-S. Wu, K. W. Leung, and J.-F. Mao, "Microstrip-fed differential dielectric resonator antenna and array," *IEEE Antennas Wireless Propag. Lett.*, vol. 17, no. 9, pp. 1736–1739, Sep. 2018.

[6] M. S. Al Salameh, Y. M. M. Antar, and G. Seguin, "Coplanar-waveguide-fed slot-coupled rectangular dielectric resonator antenna," *IEEE Trans. Antennas Propag.*, vol. 50, no. 10, pp. 1415–1419, Oct. 2002.

[7] K. W. Leung, K. M. Luk, K. Y. A. Lai, and D. Lin, "Theory and experiment of a coaxial probe fed hemispherical dielectric resonator antenna," *IEEE Trans. Antennas Propag.*, vol. 41, no. 10, pp. 1390–1398, Oct. 1993.

[8] Z. N. Chen, D. Liu, H. Nakano, X. Qing and T. Zwick, *Handbook of Antenna Technologies*. Singapore: Springer, 2016.

[9] D. Guha and C. Kumar, "Microstrip patch versus dielectric resonator antenna bearing all commonly used feeds: An experimental study to choose the right element," *IEEE Antennas Propag. Mag.*, vol. 58, no. 1, pp. 45–55, Feb. 2016.

[10] V. Hamsakutty, A. V. P. Kumar, J. Yohannan, and K. T. Mathew, "Hexagonal dielectric resonator antenna for 2.4 GHz WLAN applications," *Microw. Opt. Technol. Lett.*, vol. 49, no. 1, pp. 162–164, Jan. 2007.

[11] S. H. Ong, A. A. Kishk, and A. W. Glisson, "Rod-ring dielectric resonator antenna," *Int. J. RF Microw. Comput.-Aided Eng.*, vol. 14, no. 5, pp. 441–446, 2004.

[12] L. Huitema and T. Monediere, "Dielectric materials for compact dielectric resonator antenna applications," in *Dielectric Material*, vol. 2. Rijeka, Croatia: InTech, 2012.

[13] S. Keyrouz and D. Caratelli, "Dielectric resonator antennas: Basic concepts, design guidelines, and recent developments at millimeter-wave frequencies," *Int. J. Antennas Propag.*, vol. 2016, Oct. 2016, Art. no. 6075680.

[14] A. A. Khan, M. H. Jamaluddin, S. Aqeel, J. Nasir, J. U. R. Kazim, and O. Owais, "Dual-band MIMO dielectric resonator antenna for WiMAX/WLAN applications," *IET Microw., Antennas Propag.*, vol. 11, no. 1, pp. 113–120, Jan. 2017.

[15] A. A. Kishk and W. Huang, "Size-reduction method for dielectric-resonator antennas," *IEEE Antennas Propag. Mag.*, vol. 53, no. 2, pp. 26–38, Apr. 2011.

[16] S. Mishra, S. Das, S. S. Pattnaik, S. Kumar, and B. K. Kanaujia, "Three-dimensional cylindrical design multiple-input-multiple-output/diversity antenna with high isolation for wireless communication applications," *Int. J. RF Microw. Comput.-Aided Eng.*, vol. 30, no. 1, Jan. 2020, Art. no. e22001, doi: 10.1002/mmce.22001.

[17] R. S. Yaduvanshi and H. Parthasarathy, *Rectangular Dielectric Resonator Antennas*. New Delhi, India: Springer, 2016.

[18] R. K. Mongia and A. Ittipiboon, "Theoretical and experimental investigations on rectangular dielectric resonator antennas," *IEEE Trans. Antennas Propag.*, vol. 45, no. 9, pp. 1348–1356, Sep. 1997.

[19] A. Petosa, *Dielectric Resonator Antenna Handbook*. Boston, MA, USA: Artech House, 2007.

[20] R. K. Mongia and P. Bhartia, "Dielectric resonator antennas—A review and general design relations for resonant frequency and bandwidth," *Int. J. Microw. Millim.-Wave Comput.-Aided Eng.*, vol. 4, no. 3, pp. 230–247, Jul. 1994.

[21] A. S. Al-Zoubi, A. A. Kishk, and A. W. Glisson, "A linear rectangular dielectric resonator antenna array fed by dielectric image guide with low cross polarization," *IEEE Trans. Antennas Propag.*, vol. 58, no. 3, pp. 697–705, Mar. 2010.

[22] D. Guha, H. Gajera, and C. Kumar, "Cross-polarized radiation in a cylindrical dielectric resonator antenna: Identification of source, experimental proof, and its suppression," *IEEE Trans. Antennas Propag.*, vol. 63, no. 4, pp. 1863–1867, Apr. 2015.

[23] D. Guha, H. Gajera, and C. Kumar, "Perturbation technique to improve purity of modal fields in dielectric resonator antenna resulting in reduced cross-polarized radiation," *IEEE Trans. Antennas Propag.*, vol. 63, no. 7, pp. 3253–3257, Jul. 2015.

[24] H. Gajera, D. Guha, and C. Kumar, "New technique of dielectric perturbation in dielectric resonator antenna to control the higher mode leading to reduced cross-polar radiations," *IEEE Antennas Wireless Propag. Lett.*, vol. 16, pp. 445–448, 2017.

[25] S. Mikki and Y. Antar, *New Foundations for Applied Electromagnetics: The Spatial Structure of Electromagnetic Fields*. Norwood, MA, USA: Artech House, 2016.

[26] H. S. Singh, B. R. Meruva, G. K. Pandey, P. K. Bharti, and M. K. Meshram, "Low mutual coupling between MIMO antennas by using two folded shorting strips," *Prog. Electromagn. Res. B*, vol. 53, pp. 205–221, Jul. 2013.

[27] J. L. Volakis, *Antenna Engineering Handbook*. New York, NY, USA: McGraw-Hill, 2007.

[28] Y. K. Choukiker, S. K. Sharma, and S. K. Behera, "Hybrid fractal shape planar monopole antenna covering multiband wireless communications with MIMO implementation for handheld mobile devices," *IEEE Trans. Antennas Propag.*, vol. 62, no. 3, pp. 1483–1488, Mar. 2014.

[29] J. Zheng, X. Gao, Z. Zhang, and Z. Feng, "A compact eighteen-port antenna cube for MIMO systems," *IEEE Trans. Antennas Propag.*, vol. 60, no. 2, pp. 445–455, Feb. 2012.

[30] B. Feng, J. Lai, Q. Zeng, and K. L. Chung, "A dual-wideband and high gain magneto-electric dipole antenna and its 3D MIMO system with metasurface for 5G/WiMAX/WLAN/X-band applications," *IEEE Access*, vol. 6, pp. 33387–33398, 2018.

[31] M.-Y. Li, Y.-L. Ban, Z.-Q. Xu, G. Wu, C.-Y.-D. Sim, K. Kang, and Z.-F. Yu, "Eight-port orthogonally dual-polarized antenna array for 5G smartphone applications," *IEEE Trans. Antennas Propag.*, vol. 64, no. 9, pp. 3820–3830, Sep. 2016.

[32] S. Chen and K.-M. Luk, "A dual-mode wideband MIMO cube antenna with magneto-electric dipoles," *IEEE Trans. Antennas Propag.*, vol. 62, no. 12, pp. 5951–5959, Dec. 2014.

SHAILESH MISHRA (Member, IEEE) received the B.E. degree (Hons.) from the University of Agra, India, and the M.E. degree (Hons.) in electronics and communication engineering from the National Institute of Technical Teachers Training and Research, Chandigarh, India. He is currently pursuing the Ph.D. degree in microwave engineering with the Indian Institute of Technology, Dhanbad. He is working as an Assistant Professor with the Electronics and Communication Engineering Division, Netaji Subhas Institute of Technology, New Delhi, India. His research interests include antenna design, antenna array, metamaterial, and MIMO antennas. He is a Life Member of the Indian Society for Technical Education (ISTE).

SUSHRUT DAS (Senior Member, IEEE) received the B.Sc. degree in physics from Calcutta University, the M.Sc. degree in physics from Banaras Hindu University, the M.Tech. degree in microwave engineering from Burdwan University, and the Ph.D. degree from the Indian Institute of Technology, Kharagpur, India, in 1999, 2001, 2003, and 2007, respectively. He is currently working as an Associate Professor with the Department of Electronics Engineering, Indian School of Mines, Dhanbad. He has authored one book on *Microwave Engineering* (Oxford University Press, 2014) and published several research articles in refereed international journals and conferences. His research interests include microwave antennas, microwave passive structures, wireless energy transfer, and energy harvesting. He had received the URSI Young Scientist Award in Istanbul, Turkey, in 2011.

SHYAM SUNDAR PATTNAIK (Senior Member, IEEE) received the Ph.D. degree in engineering from Sambalpur University, India, in 1992. He worked as a Vice Chancellor of the Biju Patnaik University of Technology, Rourkela, from 2014 to 2017. He also worked at the Department of Electrical Engineering, University of Utah, USA. Since 2004, he has been a Professor and the Head of the Educational Television Center, NITTTR. He is currently working as the Director of the National Institute of Technical Teacher's Training and Research (NITTTR), Chandigarh, under the Ministry of Human Resource and Development, Government of India. He has one patent and 252 technical research publications to his credit. He has conducted number of conferences and seminars. He has published two International books and three International book chapters. His areas of interest are soft computing, information fusion, and their application to bio-medical imaging, antenna design, metamaterial antennas, and video processing. He is a Fellow of IETE, a Life Member of ISTE, and has been listed in the Who's Who in the world. He was a recipient of National Scholarship, BOYSCAST Fellowship, SERC Visiting Fellowship, INSA Visiting Fellowship, UGC Visiting Fellowship, and best paper award. Recently, he had received Certificate of Commendation for Sponsored Projects, Gold Medal (Certificate of Excellence) for the year 2018, and Leading Educationalist of India Award 2018.

BINOD KUMAR KANAUJIA (Senior Member, IEEE) received the B.Tech. degree in electronics engineering from the Kamla Nehru Institute of Technology, Sultanpur, India, in 1994, and the M.Tech. and Ph.D. degrees from the Department of Electronics Engineering, Indian Institute of Technology (Banaras Hindu University), Varanasi, India, in 1998 and 2004, respectively. He is currently working as a Professor with the School of Computational and Integrative Sciences, Jawaharlal Nehru University, New Delhi, India. He had supervised 50 M.Tech. and 15 Ph.D. scholars in the field of RF and microwave engineering. He has been credited to publish more than 280 research articles with more than 1700 citations and H-index of 18 in several peer-reviewed journals and conferences. He had successfully executed five research projects sponsored by several agencies of Government of India, such as DRDO, DST, AICTE, and ISRO. He is also a member of several academic and professional bodies, such as the IEEE, Institution of Engineers (India), Indian Society for Technical Education, and Institute of Electronics and Telecommunication Engineers of India. He is currently on the editorial board of several international journals.

• • •

SACHIN KUMAR received the B.Tech. degree in electronics and communication engineering from Uttar Pradesh Technical University, Lucknow, India, in 2009, and the M.Tech. and Ph.D. degrees in electronics and communication engineering from Guru Gobind Singh Indraprastha University, Delhi, India, in 2011 and 2016, respectively. He is currently working as a Researcher with the School of Electronics Engineering, Kyungpook National University, Daegu, South Korea. His research interests include circularly-polarized microstrip antennas, reconfigurable antennas, ultrawideband antennas, defected ground structure, and microwave components.